Adaptive Optics Systems: Lagrange-Based Woofer-Tweeter Control

Paulo Jorge Duda de Morais
University of São Paulo
São Paulo, Brazil

Rubens Cavalcante da Silva
University of São Paulo
São Paulo, Brazil

Wagner de Rossi
IPEN-CNEN/SP
São Paulo, Brazil

Cláudio Costa Motta
University of São Paulo
São Paulo, Brazil

2025 SBFoton International Optics and Photonics Conference (SBFoton IOPC) | 979-8-3315-9497-8/25/$31.00 ©2025 IEEE | DOI: 10.1109/SBFOTONIOPC66433.2025.11218600

***Abstract*—This paper presents the implementation of a Lagrange-based processor extension for woofer-tweeter adaptive optics control. The approach leverages the complementary response of two deformable mirrors to compensate for a broad range of wavefront aberrations. Applications include high-energy laser propagation through the atmosphere, where adaptive optics mitigate distortions caused by turbulence, enabling improved beam focus and reduced scintillation in scenarios such as free-space optical communication and energy transmission.**

I. Introduction

Adaptive optics (AO) refers to a set of techniques and devices used to dynamically correct wavefront distortions in optical systems caused by environmental turbulence or system aberrations. By employing real-time feedback mechanisms, usually involving wavefront sensors and deformable mirrors, AO systems restore image sharpness or beam quality degraded during propagation through inhomogeneous media. AO systems are used to correct wavefront distortions in applications such as microscopy, astronomy, and laser communications. The woofer-tweeter configuration employs two deformable mirrors: one for low-order aberrations (woofer) and one for high-order (tweeter).

This study is also motivated by the need to optimize high-energy laser (HEL) systems for long-range propagation through turbulent media. The techniques discussed in [3]–[6] show that scintillation and wavefront distortion from atmospheric turbulence are the primary limiting factors in laser beam quality. Using deformable mirrors controlled via fast wavefront sensors, such as Shack–Hartmann arrays, adaptive optics systems enable dynamic phase compensation essential for maintaining beam integrity.

II. Zernike Polynomials

Zernike polynomials are a set of orthogonal polynomials defined on the unit disk. They are widely used to represent wavefront aberrations due to their relationship with classical optical errors such as defocus, coma, and astigmatism.

Each Zernike polynomial $Z_n^m(\rho,\theta)$ is expressed in polar coordinates (ρ,θ) as:

$$Z_n^m(\rho,\theta) = R_n^{|m|}(\rho)\cdot\begin{cases}\cos(m\theta), & m\geq 0\\ \sin(|m|\theta), & m<0\end{cases} \tag{1}$$

Where $R_n^{|m|}(\rho)$ is the radial polynomial:

$$R_n^{|m|}(\rho) = \sum_{k=0}^{(n-|m|)/2}\frac{(-1)^k(n-k)!}{k!((n+|m|)/2-k)!((n-|m|)/2-k)!}\rho^{n-2k} \tag{2}$$

In practice, Zernike polynomials are commonly ordered using a single index Z_j according to the Noll sequential indexing scheme, where each index j corresponds to a specific (n,m) pair. For instance:

- Z_1: Tilt Y
- Z_2: Tilt X
- Z_3: Oblique Astigmatism
- Z_4: Defocus
- Z_5: Vertical Astigmatism
- Z_6–Z_{14}: Higher-order terms

The experiment reconstructed 14 Zernike modes from Shack-Hartmann wavefront sensor data using modal decomposition. These coefficients were obtained by projecting the measured wavefront onto the Zernike polynomial basis. This correction was performed using the woofer mirror in closed-loop mode, and the resulting coefficients are presented in the corresponding results section.

III. Mathematical Model

The Lagrange-based woofer-tweeter control model combines the influence matrices A and B of the two mirrors using control parameters. The control matrix is given by Equation 3, [1], [2]:

$$\begin{bmatrix}X\\Y\end{bmatrix} = g\begin{bmatrix}\xi A^TA+\lambda_1 I_1 & \xi\beta A^TB\\ \xi\beta B^TA & \beta^2B^TB+\lambda_2 I_2\end{bmatrix}^{-1}\begin{bmatrix}\xi A^T\\ \beta B^T\end{bmatrix}S \tag{3}$$

Where:

- A, B: influence matrices of woofer and tweeter.
- λ_1, λ_2: damping factors.
- β, ξ: Lagrange multipliers.
- g: control gain.

IV. Experimental Setup

This section describes the main components used in the experimental implementation, with emphasis on the deformable mirrors and wavefront sensor.

A. Deformable Mirrors

The woofer mirror used is the Thorlabs DMH40, a piezoelectric deformable mirror with 40 independently controlled segments. It features a 14 mm pupil diameter and is optimized for generating precise wavefront shapes using Zernike modes. The mirror achieves a physical stroke of up to ±17.6 μm of each mirror segment and supports fast closed-loop control with response times of 0.5 ms. Its integrated high-voltage drivers and USB interface make it suitable for dynamic adaptive optics applications.

The tweeter mirror is a Boston Micromachines Multi-DM, featuring 140 microelectromechanical (MEMS) actuators arranged in a square array. It is designed for high-speed correction of high-order aberrations with small strokes (up to 3.5 μm) and a resolution of about 0.25 nm. Its bandwidth supports correction rates above 1 kHz.

B. Wavefront Sensor

The wavefront sensor used is a Shack-Hartmann sensor capable of high-resolution wavefront reconstruction. It employs a microlens array to segment the incoming wavefront and measures the centroid displacements on a CMOS camera capable of providing frame rates as high as 880 fps. The acquired signal is then processed to estimate the wavefront phase, which is used as input S in the control equations.

C. Light Source

The light source (LS) used in the experiment is a Collimated Laser Diode Module. It emits at a typical wavelength of 635 nm, with an optical output power of 1.2 mW and a circular beam shape of approximately 2.9 mm in diameter.

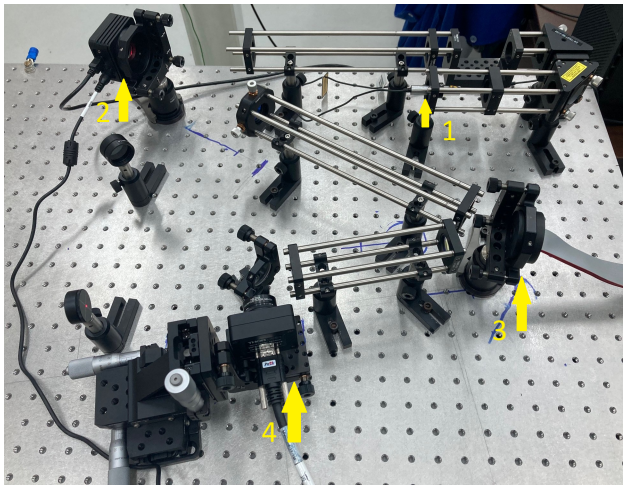

Fig. 1. Experimental setup. Components: (1) light source at 635 nm; (2) Woofer deformable mirror (Thorlabs DMP40); (3) Tweeter deformable mirror (Boston Micromachines Multi-DM); (4) Shack-Hartmann wavefront sensor.

V. Results

The system was initialized according to the experimental setup shown in Figure 1. The control architecture includes a pair of woofer-tweeter and a Shack-Hartmann wavefront sensor illuminated by a LS at 635 nm.

The software was then calibrated using wavefront sensor data. The calibration process determined the input vector S used in Equation 3 for the control law.

The initial open-loop wavefront measured before correction is illustrated in Figure 2. The measured surface presents a peak-to-valley (P-V) amplitude of 17.443μm, a mean amplitude of -8.598μm, and an RMS amplitude of 4.955μm.

Based on this measurement, the control system was calibrated using the wavefront sensor data. The parameters obtained for Equation 3 were as follows:

- $\lambda_1 = 29.12386$ (woofer damping factor)
- $\lambda_2 = 106.36$ (tweeter damping factor)
- $\beta = 0.01$ (original Lagrange multiplier)
- $\xi = 1.00$ (additional Lagrange multiplier)
- $g = 1.00$ (control gain)

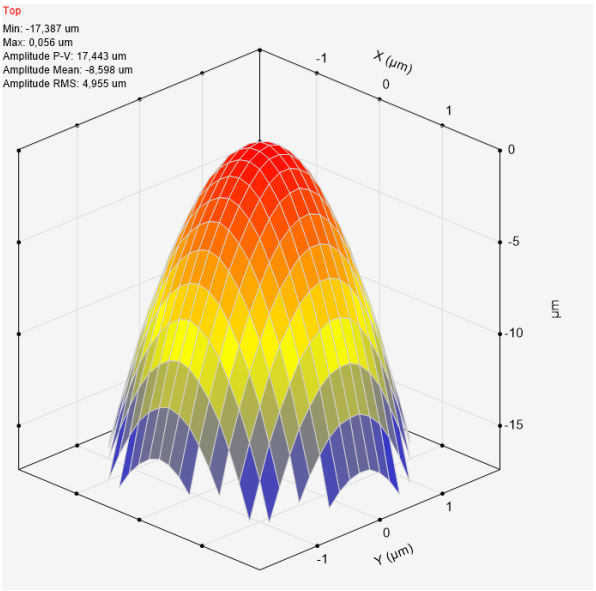

Fig. 2. Reference wavefront (open-loop): P-V amplitude = 17.443μm, Mean = -8.598μm, RMS = 4.955μm.

After control system calibration using the values presented previously ($\lambda_1 = 29.12386$, $\lambda_2 = 106.36$, $\beta = 0.01$, $\xi = 1.00$, $g = 1.00$), the control algorithm takes as input the reference wavefront from the light source, as shown in Figure 2.

Figure 3 shows the corresponding wavefront in open-loop configuration. In this condition, the system operates without correction, which means that the command vectors X and Y in Equation 3 are set to zero. This surface represents the natural distortion measured by the wavefront sensor without compensation.

The figure reveals a peak-to-valley (P-V) amplitude of 1.069μm, a mean amplitude of -0.497μm, and an RMS amplitude of 0.288μm.

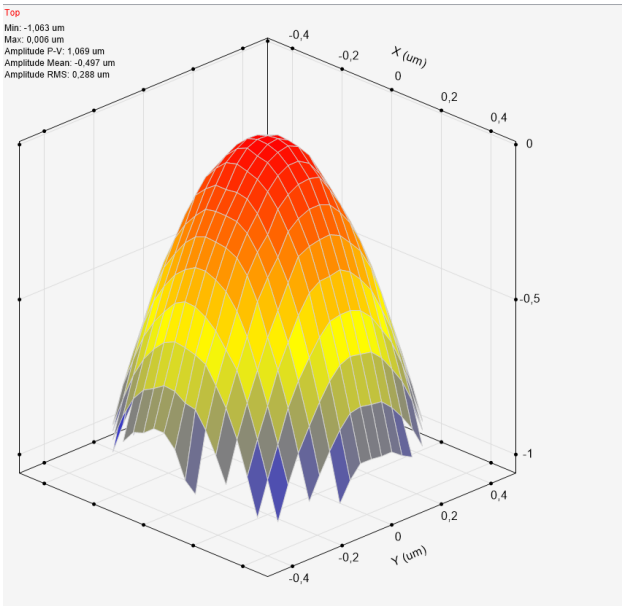

Fig. 3. Open-loop wavefront without correction: P-V amplitude = 1.069μm, Mean = -0.497μm, RMS = 0.288μm.

The closed-loop control was then activated, and the system stabilized within milliseconds. According to the model presented in Equation 3, the resulting Zernike coefficients were computed as follows:

TABLE I
ZERNIKE POLYNOMIAL COEFFICIENTS

Index	Zernike Term	Value (μm)
Z1	Tilt Y	0.000317
Z2	Tilt X	-0.006523
Z3	Ast45	-0.003403
Z4	Defocus	0.009724
Z5	Ast0	0.004665
Z6	TreY	0.001249
Z7	ComX	-0.000141
Z8	ComY	-0.004891
Z9	TreX	-0.001429
Z10	TetY	-0.000744
Z11	Sec. AstY	0.002821
Z12	SAb3	0.000165
Z13	Sec. AstX	0.000209
Z14	TetX	0.000986

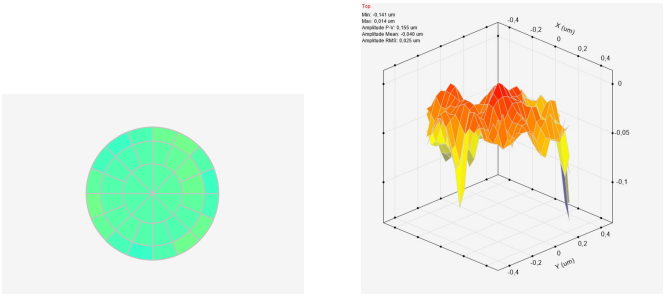

Fig. 4. Actuator profiles of the woofer (left) and tweeter (right) mirrors under closed-loop operation.

Figure 5 presents the corrected wavefront in the sensor after the closed-loop control was applied. Compared to the uncorrected result in Figure 3, the P-V, mean, and RMS amplitudes show a significant reduction, indicating that the measured wavefront closely approximates the reference wavefront shown in Figure 2.

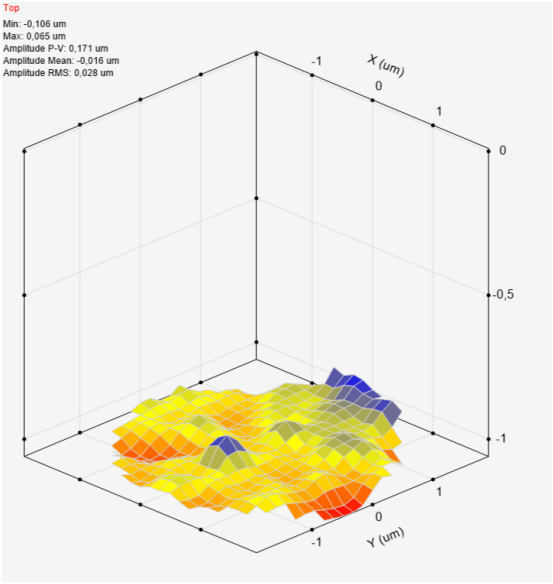

Fig. 5. Closed-loop wavefront after correction: P-V amplitude = 0.155μm, Mean = -0.040μm, RMS = 0.025μm.

VI. CONCLUSION

The Lagrange-based processor extension enables efficient control of woofer-tweeter AO systems by balancing the response of both deformable mirrors. Experimental results demonstrated significant wavefront correction, achieving sub-micron residual error levels.

This architecture is particularly promising for applications requiring rapid correction in the presence of atmospheric turbulence, such as in high-energy laser propagation, space communication, and optical energy transfer systems. Future work may include integration with real-time atmospheric modeling using phase screen techniques to further improve correction bandwidth and robustness.

REFERENCES

[1] W. Zou et al., "Woofer-tweeter adaptive optics scanning laser ophthalmoscopic imaging based on Lagrange-multiplier damped least-squares algorithm," *Biomedical Optics Express*, 2011.
[2] W. Zou et al., "Wavefront-aberration sorting and correction for a dual-deformable-mirror adaptive-optics system" *Optics Letters*, 2008.
[3] P. Sprangle et al., "High-power lasers for directed-energy applications," *Applied Optics*, vol. 54, no. 31, pp. F201–F209, 2015.
[4] P. J. D. de Morais et al., "Numerical solution of atmospheric laser beam propagation using artificial compressibility and pseudo-spectral methods," *SBFoton IOPC*, 2022.
[5] L. C. Andrews and R. L. Phillips, "Laser beam propagation through random media," 2nd ed., SPIE Press, 2005.
[6] P. J. D. de Morais et al., "Scintillation reduction using deformable mirrors in turbulent propagation," *SBMO/IEEE MTT-S International Microwave and Optoelectronics Conference (IMOC)*, 2023.